Fourth International Conference on Computational Plasticity (COMPLAS IV)
Barcelona, 3-6 Abril 1995

NUMERICAL ANALYSIS OF STRAIN LOCALIZATION IN CONCRETE SPECIMENS UNDER DIFFERENT LOADING PATHS

Francisco J. Martínez(*), Jose M. Goicolea(*) and Michael Ortiz(**)
(*) E.T.S. Ingenieros de Caminos. Universidad Politécnica de Madrid
(**) Division of Engineering. Brown University

Abstract

This work addresses the characterization and modelling of the softening phase in the mechanical behaviour of mass concrete under compression. The interpretation of softening is related to the interaction between microstructural components of the material, which results in the generation of non homogeneous strain states where deformations are localized in relatively thin bands.

The objective here is to analyze the influence of the loading path, considering various biaxial and uniaxial combinations. With this in mind a mixture model has been employed to simulate the behaviour of concrete. The model includes two phases: the aggregate represented with a cohesive-frictional elastoplastic material with a non-associative flow rule and the matrix considered to be an elastic-brittle material.

The application of the model to different tests reproduces well some aspects of the initiation and development of the localization bands, leading to a consistent interpretation of the failure of concrete specimens under compression as a structural mechanism.

1 PREAMBLE

Experimental evidence confirms that mass concrete, when deformed sufficiently into the plastic range, gives way to highly localized deformation patterns, in the form of shear bands [17], [16], [20]. This leads to a non-uniform state of deformation and a markedly softening response prior to failure. A similar behaviour is observed in other geological or so-called cohesive-frictional materials.

In our view, many aspects of the softening behaviour of concrete under compression can be explained from its heterogeneous nature, being composed of two distinct phases: mortar and aggregate. High stress concentrations arise in the mortar-aggregate interface, generating microcracks or defects around the grains. These microcracks activate the subsequent crack growth when concrete is loaded. At these early stages, crack growth is a fairly distributed process. For certain stress paths these microcracks tend to be confined into narrow bands which eventually form well defined failure planes. Therefore one can conclude that fracture is the phenomenon which governs the strain localization process in concrete.

The numerical treatment of strain localization by finite elements involves important challenges, such as modelling a discontinuity in the strain field and the ill-posedness of the boundary value problem when softening is present.

In spite of some sucessful attempts to reproduce numerically localization processes in granular materials, no realistic comprehensive model for macroscopic compressive failure of quasi-brittle materials, such as concrete, has been presented. Most of the models are continuum-based and do not take into account the localization of deformations caused by strain softening. In these cases the parameters need to be fitted directly to test results including softening as an intrinsic property.

Other approaches tend to represent the concrete at a very low scale by means of micromechanical models [12], [14], [20]. These models have shown quite realistic results with the main drawback of the computer resources needed to provide these.

The approach employed in this work attempts to provide a bridge between the continuum and micromechanical models. With this aim, we will show that, with an adequate representation of the mortar as an elastic-brittle material and the aggregate as a granular medium, by means of the theory of mixtures, it is possible to reproduce localized failure modes in concrete under compressive states of stress. In the remaining of this paper, firstly we summarize the assumptions made, regarding the mixture model and the representation of each phase. This model has been applied previously to simulate with *numerical experiments* the uniaxial compressive failure of prismatic plain concrete specimens, varying the size of the specimens and the boundary conditions [7]. Secondly, in this work, the application of the model have been extended to multiaxial states of stress. The results show that the proposed model is able generally to reproduce the experimentally observed failure modes.

2 DESCRIPTION OF THE MODEL

Concrete can be idealized as a composite material as was firstly advocated by Ortiz and Popov [8]. Mixture theory is a particularly convenient way of taking into account the strong heterogeneity of concrete, by considering two main phases: mortar and aggregate. A consequence of this assumption is that externally applied stresses distribute unequally between the two phases. The average stresses acting in mortar and aggregate must jointly equilibrate the applied loads, but may be vastly different from each other, due to the difference in the mechanical behaviour of the two components. It seems reasonable to assume that these phase stresses drive the inelastic mechanisms of cracking in mortar and plastic flow in aggregate. In other words, the inelastic mechanisms are driven by stresses which may differ substantially from the applied (nominal) values.

Mixture theories provide a simple yet effective means of estimating the value of the phase stresses. They may give rise to prediction that purely compressive uniaxial loads induce large tensile stresses in mortar which act normal to the axis of loading.

This theory relies on the main assumption that an arbitrarily small volume of concrete contains both aggregate and mortar in fixed volumetric fractions α_1 and α_2 respectively. The conservation laws for a mixture may be obtained by requiring certain invariance properties from an energy balance equation (see Ortiz and Popov [8] and Martinez [6] for a detailed discussion).

The equilibrium requirement may be expressed as:

$$\boldsymbol{\sigma} = \alpha_1 \boldsymbol{\sigma}_1 + \alpha_2 \boldsymbol{\sigma}_2, \tag{1}$$

where $\boldsymbol{\sigma}_1$ and $\boldsymbol{\sigma}_2$ denote the average (phase) stresses acting in aggregate and mortar respectively, and $\boldsymbol{\sigma}$ the applied (global) stresses. It should be remarked [9], that $\boldsymbol{\sigma}_1$ and $\boldsymbol{\sigma}_2$ have to be understood in the sense of the theory of interacting continua; the phase stresses are macroscopic variables pertaining to material neighbourhoods which are large compared to the microstructure.

The absence of diffusion between the phases necessitates compatibility of macroscopic deformations, that is:

$$\boldsymbol{\varepsilon} \equiv \boldsymbol{\varepsilon}_1 = \boldsymbol{\varepsilon}_2, \tag{2}$$

where $\boldsymbol{\varepsilon}_1$, $\boldsymbol{\varepsilon}_2$ and $\boldsymbol{\varepsilon}$ denote the macroscopic strain tensors of aggregate, mortar and concrete respectively. As in the case of phase stresses, a similar remark applies to the nature of the strain tensors, which are not intended as measures of the deformation processes that take place at the microscopic level.

Under these two main assumptions: composition rule (1) and compatibility condition (2), the overall stress-strain relations for concrete can be obtained from those of its constituents. It is then possible to relate $\boldsymbol{\sigma}_1$ and $\boldsymbol{\sigma}_2$ with the concrete stress $\boldsymbol{\sigma}$ as follows:

$$\boldsymbol{\sigma}_1 = \boldsymbol{B}_1 : \boldsymbol{\sigma} + \boldsymbol{\rho}_1, \tag{3}$$

$$\boldsymbol{\sigma}_2 = \boldsymbol{B}_2 : \boldsymbol{\sigma} + \boldsymbol{\rho}_2, \tag{4}$$

where $\boldsymbol{B}_1$ and $\boldsymbol{B}_2$ are the influence tensors and $\boldsymbol{\rho}_1$ and $\boldsymbol{\rho}_2$ the residual stresses, whose exact meaning is detailed elsewhere ([8], [9] and [6]).

2.1 Representation of aggregate as a granular material

The aggregate phase may be idealized as a set of granular particulates which interact by means of contact forces exerted between each other, similarly to cohesionless soils. The constitutive behaviour and the strength capacity is mainly governed by the level of average pressure. A plastic criterion which has been frequently used to characterize the failure of cohesionless soils is the Drucker-Prager condition which can be expressed as:

$$\mathcal{F} \equiv \sqrt{J_2} + \alpha I_1 - \kappa_p, \tag{5}$$

where $I_1 = \sigma_{ii}$ (first invariant of the stress tensor) and $J_2 = \frac{1}{2} s_{ij} s_{ij}$ (second invariant of the stress deviators).

The coefficients α and κ_p are related to the material friction angle Φ and the cohesion c respectively. They may be obtained by fitting the Drucker-Prager criterion to the Mohr-Coulomb hypothesis, enforcing the coincidence of the compression meridians for both criteria.

Another distinct characteristic of granular materials is the fact that the dilatancy angle Ψ, defined as the ratio between the volumetric and deviatoric plastic strain rates, does not in general coincide with the internal friction angle Φ. This leads to consider a flow potential of the type:

$$\mathcal{G} \equiv \sqrt{J_2} + \beta I_1, \tag{6}$$

where β is a function of the dilatancy angle Ψ. The plastic strain rates are then given by:

$$\dot{\boldsymbol{\varepsilon}}^p = \dot{\gamma} \frac{\partial \mathcal{G}(\boldsymbol{\sigma})}{\partial \boldsymbol{\sigma}}, \tag{7}$$

where $\dot{\gamma}$ is the plastic consistency parameter.

A hardening evolution law for α has been adopted, very similar to the expression advocated by Vermeer and Borst [19] and Leroy and Ortiz [5]:

$$\left.\begin{aligned} \alpha(\bar{\varepsilon}_p) = \alpha_0 + (\alpha_{sat} - \alpha_0)\sqrt{1 - \frac{[\bar{\varepsilon}_p - (\bar{\varepsilon}_p)_{sat}]^2}{(\bar{\varepsilon}_p)_{sat}^2}} & \quad \bar{\varepsilon}_p \leq (\bar{\varepsilon}_p)_{sat}. \\ \alpha(\bar{\varepsilon}_p) = \alpha_{sat} & \quad \bar{\varepsilon}_p \geq (\bar{\varepsilon}_p)_{sat}. \end{aligned}\right\} \tag{8}$$

Thus, the friction angle Φ will be increased monotonically from Φ_0 to Φ_{sat} as a function of the effective plastic strain.

2.2 Representation of mortar as an elastic-brittle material

The mortar phase provides cohesion to the granular phase. A distinct characteristic of concrete is that its elastic properties degrade as a consequence of microcrack extension in mortar. This microcrack extension originates an anisotropic constitutive behaviour in concrete. In the present formulation mortar is idealized as a elastic material with some criteria to define the crack propagation.

Different numerical approaches have been proposed to represent the brittle behaviour in concrete: the fictitious crack model of Hillerborg [3], the crack band model proposed by Bazant [1], etc. Most of the existing smeared crack models have difficulties in representing correctly the final stage of mode-I separation. An excessively stiff response is found generally, due to stress locking resulting from the assumption of displacement continuity, excessive shear stress transfer along the crack, and other factors [13].

An alternative to overcome the above deficiency of the smeared approach is to remove finite elements from the mesh. Element removal as a procedure for advancing cracks through a finite element mesh has been employed previously by Ortiz and Giannakopoulos [11] in crack propagation in monolithic ceramics under mixed mode loading. More recently Rots has employed a similar technique applied to concrete [13].

In the present approach, it is assumed that the fracture energy is entirely determined by the conditions existing at the tip of the crack. Therefore, it seems reasonable to expect the conditions for crack growth to be a function of the near-tip stress intensities. In keeping with this assumption postulated by Ortiz and Giannakopoulos [11], a fracture criterion can be defined of the following form:

$$\mathcal{G}^e = \mathcal{G}^c \tag{9}$$

where $\mathcal{G}^e$ is the energy release rate due to an extension of a crack and $\mathcal{G}^c$ is a material constant called critical energy release rate.

It is sought to remove elements in such a way as to satisfy fracture criterion (9). Consider for simplicity, a square finite element mesh of grid of size h, containing an element-wide preexisting crack. Let Ω_e denote the domain of a generic element. The energy release rate due to its removal may be estimated as follows:

$$\mathcal{G}^e_{\Omega_e} \approx \frac{1}{h}\int_{\Omega_e} \frac{1}{2} D_{ijkl}\varepsilon_{ij}\varepsilon_{kl} d\Omega_e. \tag{10}$$

The criterion adopted for eliminating an element from the mesh is:

$$\mathcal{G}^e_{\Omega_e} \geq \mathcal{G}^c. \tag{11}$$

For isoparametric quadrilaterals the integral in (10) may be approximated by a one point quadrature rule as:

$$\mathcal{G}^e_{\Omega_e} \approx W_e h, \tag{12}$$

where $W_e = \frac{1}{2} D_{ijkl} \varepsilon_{ij} \varepsilon_{kl}$ is the strain energy density at the centroid of the element.

In practice, in this work a slight modification of this criterion has been used. This consists in enforcing equation (12) for the control volume of one Gauss-point. As 3D brick elements with $2 \times 2 \times 2$ integration are employed, equation (12) is modified to read $\mathcal{G}^e_{\Omega_e} = W_e h/8$.

3 RESULTS

The above material model and mixture theory have been coded as a user-defined material within the general purpose nonlinear finite element code ABAQUS [4], and employed to perform *numerical experiments*. The intention is to reproduce different biaxial compression tests of concrete specimens, attempting to verify whether with such simple constitutive model for the mortar and aggregate, it is possible to represent the basic failure mechanisms under multiaxial loading paths.

Square elements of 5 mm length have been adopted for the whole model. In this fashion, the element size provides a characteristic length representing an average size of the aggregate. We assume the existance of critical defects consisting of interfacial cracks between the mortar and aggregate triggering the initiation of the cracking process. In all of the analyses the existance of a critical microcrack at the center of the specimen has been assumed.

From the numerical standpoint, special attention has been dedicated to the integration of the Drucker-Prager plasticity, for which a return-mapping algorithm has been employed. The difficulty associated with it is due to the vertex on the hydrostatic axis, corresponding to failure by cavitation. The presence of the vertex may render the state update procedure ill-posed or even undefined when the confining pressure is small. To overcome these problems, the corner has been rounded off by fitting a spherical cap of the same form as advocated by Leroy and Ortiz [5] (see [6] for a more detailed discussion).

Hugues' $\overline{B}$-method was adopted to preclude locking due to near-incompressibility under fully developed plastic flow. The modified-Riks or arc-length method has been adopted for displacement and force control.

The parameters used for idealizing the mortar are: Young's modulus $E_{mortar} = 25\,\text{GPa}$, Poisson coefficient $\nu = 0.2$, Fracture energy $\mathcal{G}^c = 160$ J/m^2 and volumetric fraction $\alpha_{mortar} = 0.15$. Aggregate is characterized by the following parameters: $E_{aggregate} = 40$ GPa, $\nu = 0.2$, friction angle

$\Phi_0 = 20°$, $\Phi_{sat} = 30°$ ($\bar{\varepsilon}_p \geq 0.5\%$), dilatancy $\Psi = 10°$, cohesion $c = 0.4$ MPa and volumetric fraction $\alpha_{aggregate} = 0.85$.

The specimens modelled are prismatic cubes of $100mm$ length. The load conditions correspond to three different stress paths, according to the experimental configurations defined by Van Mier in [17]. We designate by 2 the main compressive loading axis (vertical in the figures), 1 the transverse axis (horizontal in the figures) and 3 the remaining transverse axis (perpendicular to the plane of the figures). The three stress-paths are achieved by imposing the following constant displacement-ratio paths: $\Delta l_3/\Delta l_2$ $-0.33/-1.0$ (biaxial), $-0.10/-1.0$ (biaxial), $0.0/-1.0$ (uniaxial plane strain compression), where Δl_i is the prescribed displacement along axis i.

Figure 1 shows the evolution of the cracking process in the mortar for the first biaxial stress path, while figure 2 depicts the case of uniaxial compression.

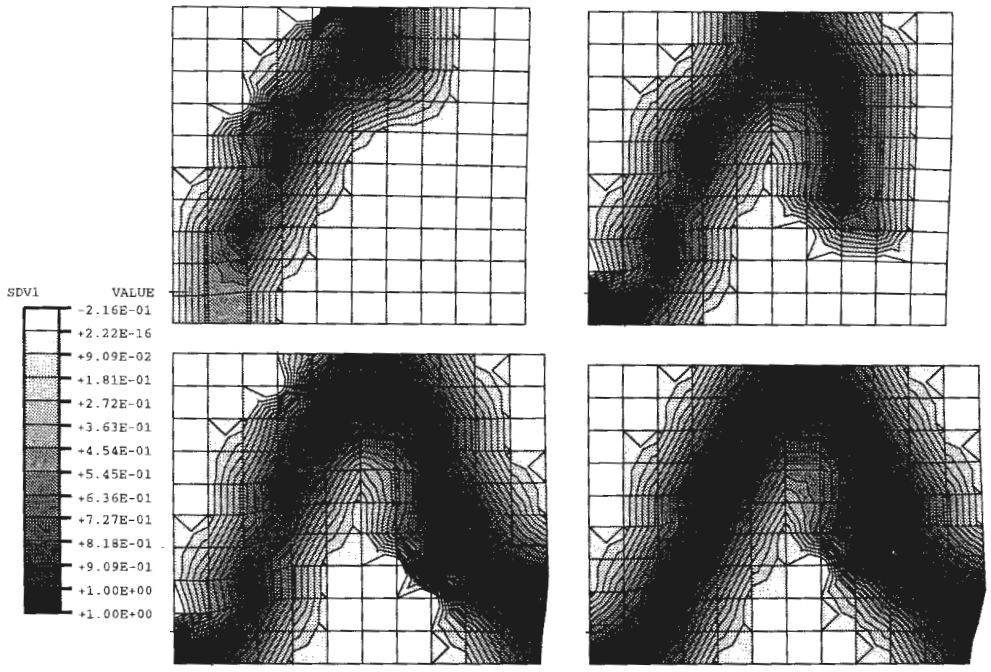

Figure 1: Sequence of deformed shapes (displacements magnified $\times 25$) for the case of biaxial loading ($\Delta l_3/\Delta l_2 = -0.33/-1.0$). The fringe levels indicate the cracking process in the mortar, indicative of the evolution of the localised shear band.

It is clear from these figures that the orientation of the localisation band is markedly different in both cases. It is also clear that the overall specimen response is governed by a "structural" deformation involving displacements of rigid, intact areas along shear bands, rather than by a softening stress-

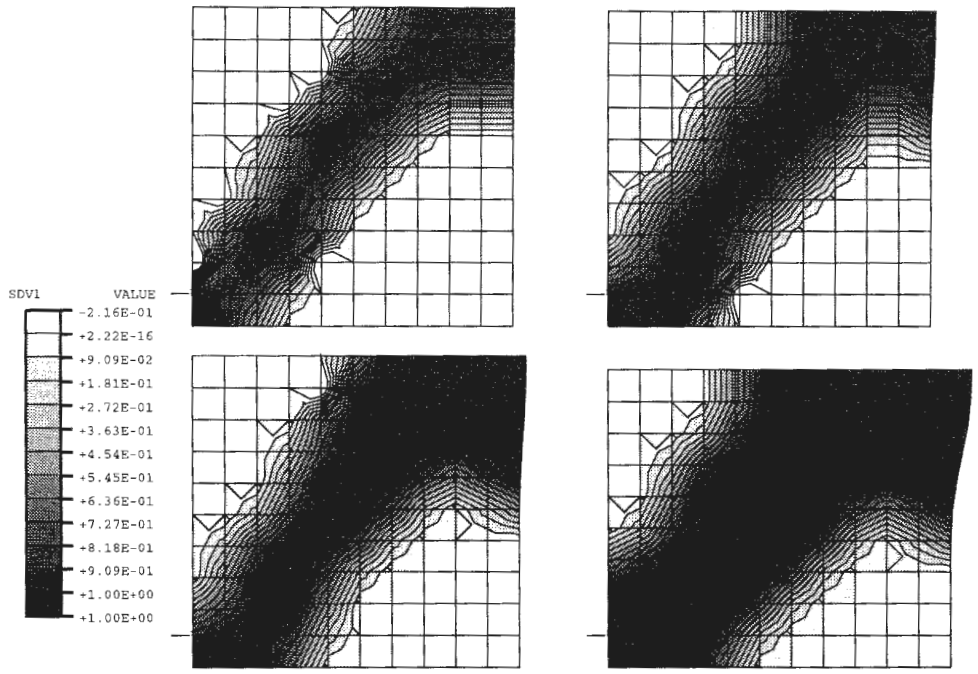

Figure 2: Sequence of deformed shapes (displacements magnified $\times 2$) for the case of uniaxial plane strain compression ($\Delta l_3/\Delta l_2 = 0.0/-1.0$). The fringe levels indicate the cracking process in the mortar, indicative of the evolution of the localised shear band.

strain law.

There are two interacting mechanisms which govern the devolopment of the cracking in the mortar and consequently the formation of the shear band in the aggregate. On one hand, the dilatancy associated with the shearing of the aggregate phase: due to the volumetric compatibility condition between the two phases, the increase of volume of the aggregates generates high tensile stresses in the mortar. On the other hand, during microcrack extension in the mortar a phenomenon of stress relief is produced. Hence high hydrostatic tensile stresses are transfered to the aggregate, causing it to fail by cavitation, leading in turn to an increase of the dilatancy. This feed-back mechanism drives the localization process in concrete due to its heterogeneous composition.

The mean stress - mean strain curve for the three loadings is represented in figure 3. These curves represent the global "structural" response of the specimens, based on the development of the shear bands. As soon as the shear band links up with the surface of the specimen, the curve suffers an abrupt drop from the level of the uniform solution, exhibiting a markedly softening response. It must be said that the softening branch obtained here (notice the curve in some cases presents a backward slope, causing

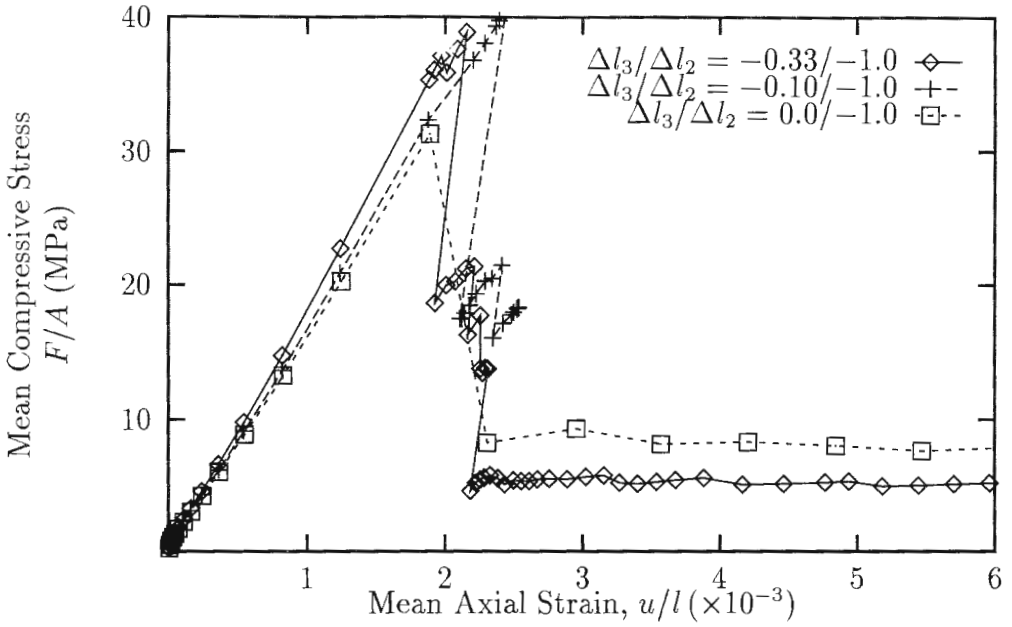

Figure 3: Mean axial stress vs. mean axial strain curves for two different biaxial load paths and uniaxial plane strain compression

numerical difficulties which were solved by continuation techniques based on arc-length methods) is steeper than the values reported in experiments. However it is important to emphasize that the softening branch is quite sensitive to the boundary conditions imposed by the friction between the loading platens and the specimen [20]. Another important factor is the stiffness of the loading system. These numerical simulations are carried out under the assumption of frictionless, rigid platens.

The comparison of the three curves (figure 3) confirms the experimental evidence [17] of an increase of the peak load of the order of 25% in the biaxial tests with respect to the uniaxial compression tests. The lower plateau is mainly governed by the strength capacity of the aggregate and consequently determines the residual strength of mass concrete. A striking result of our calculations is that the residual capacity in the uniaxial compression test is greater than in the biaxial tests. This apparent discrepancy with experiments can only be explained by the structural behaviour of the specimen as a consequence of the different orientation of the shear bands, evident from a comparison of figures 1 and 2. An estimate of the ultimate compressive stress $\bar{\sigma}$, in the idealized case of an unbounded granular medium transversed by a straight shear band of constant thickness and orientation θ, is [10]:

$$\bar{\sigma} = \frac{c\,\alpha\cot\Phi}{(\sqrt{3}\sin\theta - \alpha\cos\theta)\cos\theta} \tag{13}$$

Measuring the obtained orientation of the shear bands for biaxial ($\Delta l_3/\Delta l_2 = -0.33/-1.0$) and uniaxial tests, the ultimate stresses produced by equation (13) are respectively 2 and 3 MPa. These values indicate the critical influence of the mode of failure in the post peak response.

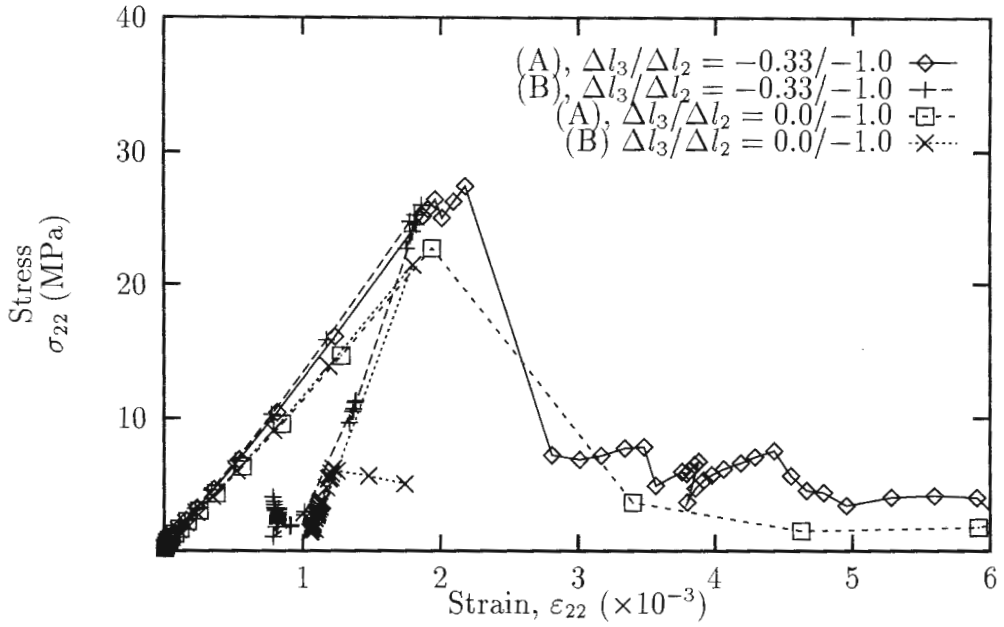

Figure 4: Axial stress vs. axial strain paths for points in two different areas within the specimen: (A) outside of fracture band, (B) within fracture band, in biaxial loading and uniaxial plane strain compression

Finally, figure 4 depicts the stress-strain curves of points in different regions of the specimen, corresponding to zones inside and outside of the shear band. The results show the inhomogeneous response inside the specimen: a softening branch is obtained in the stress-strain curve in areas close to the shear band, while the rest of the specimen unloads elastically. This confirms the interpretation that the specimen behaves, beyond the peak load, like rigid blocks shearing off along the bands.

4 CONCLUSIONS

- The most distinctive characteristic of quasi-brittle materials such as concrete under compression is that the localization processes are closely related with the fracture of the mortar phase. This phenomenon originates non-homogeneous states of deformation with a marked softening response beyond the peak stress.

- The proposed mixture model, which represents each phase of concrete (mortar and aggregate) with simple and well established constitutive

models, appears to be capable of representing axial splitting cracks and shear band failure in plain concrete under compression.

- The deformation state in concrete specimens under multiaxial compression is markedly non-homogeneous beyond the peak stress. The deformation patterns and shear bands predicted by the numerical simulations are in close agreement with experiments. The results indicate that the specimen behaves, beyond the peak load, like rigid blocks shearing off along the bands. It is the structural behaviour of this mechanism and, consequently, the mode of failure, what mainly governs the post peak load-displacement response.

- Further research into this area must address the issue of obtaining a more realistic smooth response, adjusting aspects such as the critical defects and the cracking criterion, while maintaining the simplicity of the basic constitutive assumptions.

REFERENCES

[1] BAZANT, Z. P. Mechanics of distributed cracking. Appl. Mech. Rev. Vol 39. No 5. pp 675-705. 1986.

[2] BAZANT, Z. P. y OZBOLT, J. C. Compression failure of quasibrittle material: Nonlocal microplane model. J. Eng. Mech. Vol 118. No 3. ASCE. 1992.

[3] HILLERBORG, A; MODEER, M. and PETERSSON, P. Analysis of crack formation and crack growth in concrete by means of fracture mechanics and finite elements. Cem. and Concr. Res. Vol 6. No 6. pp 773-782. 1976.

[4] HIBBITT, KARLSSON & SORENSEN. *ABAQUS User's manual, Version 5.3.* HKS, Inc. Pawtucket, Rhode Island. 1993.

[5] LEROY, Y. and ORTIZ, M. Finite element analysis of transient strain localization phenomena in frictional solids. Int. J. for Num. and Analyt. Meth. in Geomech. vol 14. pp 93-124. 1990.

[6] MARTÍNEZ, F. *Análisis de fenómenos de localización de deformaciones en materiales cohesivo-friccionales.* Tesis Doctoral. Universidad Politécnica de Madrid. 1993.

[7] MARTÍNEZ, F., GOICOLEA, J.M., ORTIZ, M. Numerical analysis of strain localization in concrete specimens. Proc. EURO-C 1994. *Computational Modelling of Concrete Structures.* Insbruck. 1994.

[8] ORTIZ, M. and POPOV, E. P. Plain concrete as a composite material. Mech. of Mat. 1. pp 139-150. 1982.

[9] ORTIZ, M. A constitutive theory for the inelastic behavior of concrete. Mech. of Mat. 4. 67. 1985.

[10] ORTIZ, M; LEROY, Y.and NEEDLEMAN, A. A finite element method for localized failure analysis. Comp. Meth. in Appl. Mech. and Eng. 61. pp 189-214. 1987.

[11] ORTIZ, M. and GIANNAKOPOULOS, A. E. Crack propagation in monolithic ceramics under mixed mode loading. Int. J. of Fract. 44. pp 233-258. 1990.

[12] ROELFSTRA, P. E; SADOUKI, H. and WITTMANN, F. H. Le béton numérique. Mat. et Cons. 107. pp 327-335. 1985.

[13] ROTS, J. G. Removal of finite elements in smeared crack analysis. Proc. 3rd. Int. Conf. on Comp. Plast. Barcelona. 1992.

[14] STANKOWSKI, T. Numerical simulation of failure in particle composites. Comp. & Struct. Vol 44. No 1/2. pp 459-468. 1992.

[15] STURE, S. and KO, H. Y. Strain-softening of brittle geologic materials. Int. J. Num. and Anal. Meth. in Geomech. Vol 2. pp 237-253. 1978.

[16] TORRENTI, J. M; DESRUES, J; BENAIJA, E. H. and BOULEY, C. Stereophotogrammetry and localization of concrete under compression. J. Eng. Mech. Vol 117. No 7. pp 1455-1465. ASCE. 1991.

[17] VAN MIER, J. G. *Strain softening of concrete under multiaxial loading conditions.* Phd Thesis. Technische Hogeschool Eindhoven. 1984.

[18] VARDOULAKIS, I. Shear band inclination and shear modulus of sand in biaxial tests. Int. J. Num. and Analyt. Meth. Geomech. Vol 4. pp 103-119. 1980.

[19] VERMEER, P. A. and BORST, R. *Non-associated plasticity for soils, concrete and rocks.* Heron. Vol 29. No 3. Delft. 1984.

[20] VONK, R. A. *A micromechanical investigation of softening of concrete loaded in compression.* Heron. Vol 38. No 3. 1993.